Efficient Green Electrophosphorescence with Al Cathode Using an Effective Electron-Injecting Polymer As the Host

Zhao Chen, QiaoLi Niu, Yong Zhang, Lei Ying, JunBiao Peng, and Yong Cao*

Institute of Polymer Optoelectronic Materials and Devices, Key Lab of Specially Functional Materials of the Ministry of Education, South China University of Technology, Guangzhou 510640, P. R. China

ABSTRACT Efficient green phosphorescent polymer light-emitting diodes (PLED) based on aluminum (Al) cathode were demonstrated. The device composed of neutral aminoalkyl substituted polyfluorene, poly[(9,9-bis(3′-(*N*,*N*-dimethylamino)propyl)-2,7-fluorene)-alt-2,7-(9,9-dioctylfluorene)] (PFN) as the host and an Ir complex, *fac*-tris(2-(4-tert-butyl)-phenylpyridine)iridium (Ir(Bu-PPy)$_3$), as the dopant. High luminous efficiency of 35.7 cd/A and a luminance of more than 10 000 cd/m^2 were obtained. The device performance was comparable to those of the devices from (Ir(Bu-PPy)$_3$), doped into PVK as the host with a low work-function metal as cathode (such as barium and calcium). We found out that the high-performance was due to the effective electron injection from PFN/Al bilayer cathode, improved charge balance as well as significant reduction of back-transfer of excitons from Ir complex to the low-lying PFN triplet level in the PVK/PFN interface.

KEYWORDS: polymer light-emitting devices (PLED) • green electrophosphorescence • electron injection from high work-function metal • Al cathode • Ir complex • PFN • PVK • aminoalkyl-substituted polyfluorene • polyvinylcarbazole • interfacial energy transfer

INTRODUCTION

Polymer light-emitting devices (PLED) have attracted great attention because of their potential applications in large-area and low-cost full-color flat panel displays and solid-state lighting (1, 2). Significant progress in the improvement of the device performances for PLEDs based on solution processing has been made in recent years; however, the performances of PLED such as the efficiency and operating lifetime have not yet met the requirements of commercial application. To achieve highly efficient electroluminescence, charge balance is of great importance (3−7). Most of the conjugated polymers are p-type semiconductors (8), which mainly transport holes in the EL processes, and thus enhancing the electron injection and transportation is an effective way to improve the performance of PLED. Low work-function metals, such as barium (Ba) or calcium (Ca), are commonly used as cathode to enhance electron injection through efficiently reducing the barrier height at the interface of cathode and emissive polymer (1, 9, 10). The drawback of the low work-function metal cathodes is that they are extremely sensitive to oxygen and moisture, requiring an inert gas atmosphere in the fabrication and encapsulation. For this reason, many salts and oxides (alkali and alkaline earth metal salts and oxides), such as LiF, CsF, and Cs_2CO_3, have been developed as the interfacial layer between Al cathode and the emissive layer (11−13). Recently, our group demonstrated that the performances of PLEDs with high work-function cathodes (such as Al, Ag, and Au) were significantly improved by inserting a thin layer of aminoalkyl-substituted polyfluorene polyelectrolytes (PFN) and their neutral precursors between emissive polymer layer and the high work-function cathode (14−16). Recently, Xu et al. reported that efficient red phosphorescent PLED with high work-function Al as cathode could be achieved by using PFN as the host when effective electron injection was realized via PFN/Al interface (17).

In this work, we report an efficient green phosphorescent PLED with high work-function Al as cathode and blends of *fac*-tris(2-(4-tert-butyl)-phenylpyridine)iridium (Ir(Bu-PPy)$_3$) and PFN as emissive layer. The device structure in this study is ITO/PEDOT/PVK/PFN:Ir(Bu-PPy)$_3$/Al. In this system, PFN plays a dual role of both the host and electron-injection materials. Besides, it was found that the device performances were highly sensitive to the thickness of PVK interlayer. With the optimized thickness of the PVK and EL layers, the device showed a best luminous efficiency of 35.7 cd/A and maximum luminance of 17 000 cd/m^2.

EXPERIMENTAL SECTION

Molecular structures under the investigation are shown in Scheme 1. Both of the neutral aminoalkyl substituted polyfluorene, poly[(9,9-bis(3′-(*N*,*N*-dimethylamino)propyl)-2,7-fluorene)-*alt*-2,7-(9,9-dioctylfluorene)] (PFN), and the green phosphorescent Ir complex, *fac*-tris(2-(4-tert-butyl)-phenylpyridine)iridium (Ir(Bu-PPy)$_3$), were synthesized in our laboratory (15, 18). Poly(*N*-vinylcarbazole) (PVK) (M_W = 1 × 10^6 g/mol) was purchased from Aldrich and was used without further purification.

The optimum device configurations in our study are as follows:

ITO/PEDOT (60 nm)/PVK (60 nm)/PFN:Ir(Bu-PPy)$_3$ (40 nm)/Al (100 nm).

* Corresponding author. E-mail: poycao@scut.edu.cn.
Received for review August 7, 2009 and accepted November 9, 2009

DOI: 10.1021/am9005258

Scheme 1. Chemical Structures of Ir(Bu-PPy)$_3$, PFN, PVK, and PBD

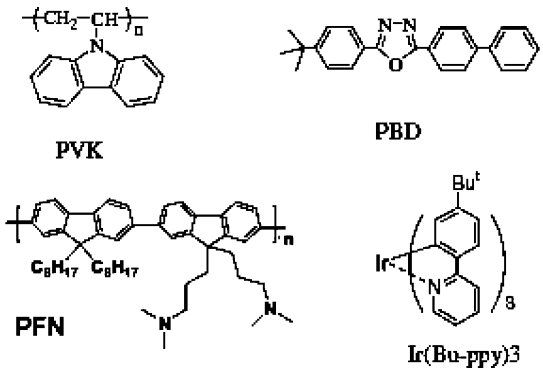

The device fabrication followed a standard procedure. The ITO substrates were cleaned in ultrasonic bath sequentially in acetone, detergent, deionized water, and isopropanol, and then baked at 80 °C for several hours. A 60 nm thick layer of poly(ethylendioxythiophene):poly(styrene sulfonic acid) (PEDOT:PSS, Baytron P4083, Bayer AG) was spin-coated onto the ITO substrate after a O_2 plasma treatment and dried in a vacuum box for 8 h. A layer of PVK (15 mg/mL) from the solution in tetrachloroethane was then spin-coated on the PEDOT and dried at 120 °C for 5 min. A mixture of Ir(Bu-PPy)$_3$ and PFN (10 mg/mL) were spin-coated from the solution of toluene. The light-emitting layer was spin-coated on the PVK layer at adopted speed to reach desired thickness. Profilometer (Tencor Alfa-Step 500) was used to measure the thickness of each layer. Finally, a more than 100 nm Al layer cathode was evaporated through a mask of 0.19 cm^2 in a vacuum chamber at a pressure of about 1×10^{-4} Pa. The evaporation rate was monitored by a crystal thickness monitor (Sycon). Except for the fabrication of the PEDOT:PSS layer, all the fabrication processes were carried out in the glovebox system with a N_2 atmosphere.

Current densities (J)—voltage (V)—luminance (L) data were collected using a Keithley 236 source measurement unit and a calibrated silicon photodiode. The luminance (cd/m^2) and luminous efficiency (cd/A) were measured by Si photodiode and calibrated by a PR-705 SpectraScan Spectrophotometer (Photo Research). PL spectra were captured by Fluorolog-3 spectrofluorimeter (Jobin-Yvon) under 325 nm light excitation and EL spectra were recorded by a CCD spectrophotometer (Instaspec 4, Oriel). External quantum efficiency (QEext) was obtained by measuring the total light output in all directions in an integrating sphere (IS080, Labsphere).

RESULTS AND DISCUSSION

Figure 1 shows the EL spectra of the PLEDs based on PFN doped with 4 wt % Ir(Bu-PPy)$_3$ with the varied PVK layer and PFN(Ir) layer thicknesses. As can be seen from Figure 1, the EL spectrum is broadened with a gradual red shift in peak position with increasing total thickness of PVK + PFN(Ir) layer. This fact suggests that a microcavity effect is dominant in determining the EL spectrum and peak position (19).

Figure 2 shows the characteristics of luminous efficiency and luminance as a function of current density for the devices with doping concentration varied from 1 to 16 wt % with fixed PVK and EL layer thickness of 60 and 40 nm, respectively. The device efficiency increased with the concentration from 1 to 4 wt %, and then decreased when

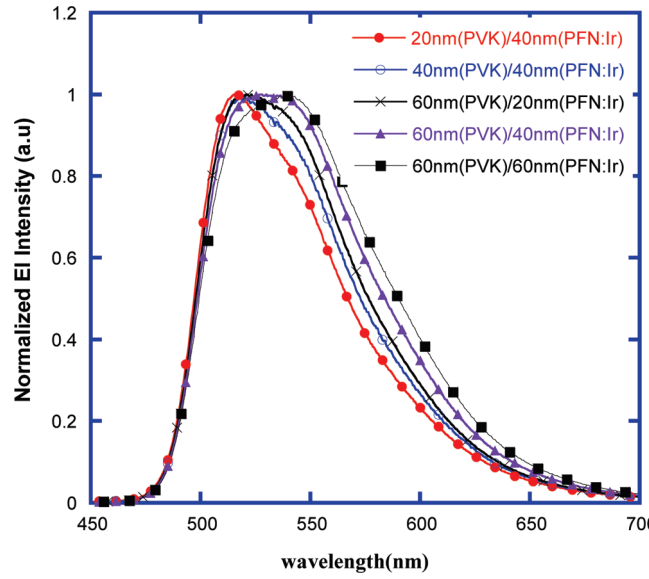

FIGURE 1. EL spectra of devices ITO/PEDOT/PVK/PFN:4 wt % Ir(Bu-PPy)$_3$/Al with PVK and PFN(Ir) layer thickness varied from 20 to 60 nm.

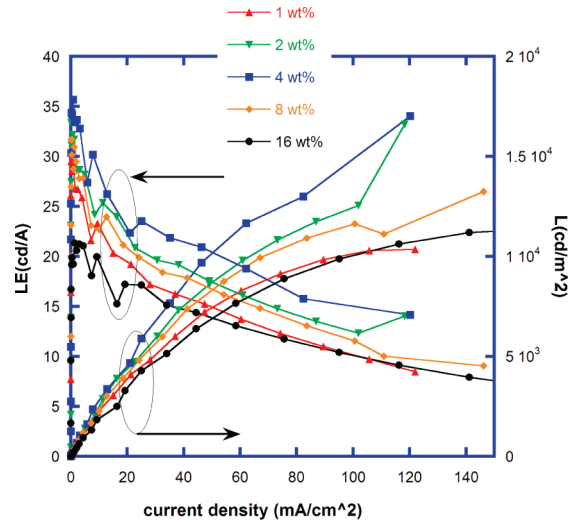

FIGURE 2. Luminous efficiency and luminance vs current density characteristics of device ITO/PEDOT/PVK (60 nm)/PFN:Ir(Bu-PPy)$_3$ (40 nm)/Al with varied doping concentrations.

doping concentration increased to 8 and 16 wt %. The device with doping concentration of 4 wt % exhibits the best performance, with a peak luminous efficiency and luminance reached as high as 35.7 cd/A and 17160 cd/m^2, respectively.

The EL performance of the device with 4 wt % doping concentration with varied PVK and active layer thickness is listed in Table 1, and the device with Ba/Al as cathode and that with 30% PBD blended into PFN are listed for comparison. As can be seen from Table 1, the device performance showed strong dependence on the thickness of the PVK layer. For the device without a PVK layer, a very poor device performance with a maximum luminous efficiency and luminance of 0.04 and 50 cd/m^2 was obtained, respectively. The device performances improved gradually with the increase in PVK layer thickness. When the PVK thickness was 20 nm, the maximum device efficiency and luminance

Table 1. EL Performance of Device with Different PVK and EL Layer Thickness in Device Configuration: ITO/PEDOT/PVK/EL/PFN:4 wt % Ir(Bu-PPy)$_3$/Al; Devices with Ba/Al Cathode and PBD Blended into PFN are Listed for Comparison

				maximum efficiency at					
cathode	PVK thickness (nm)	EL thickness (nm)	turn on voltage (V)	bias (V)	current density (mA/cm^2)	luminance (cd/m2)	LE (cd/A)	QEext (%)	maximum luminance (cd/m^2)
Al	0	40	9.0	10.3	8.8	3.6	0.04	0.02	50
Al	20	40	7.5	11.0	4.4	417	9.5	3.4	6130
Al	40	40	8.5	12.0	1.9	298	15.3	5.4	5508
Al	60	40	9.0	12.0	0.7	266	35.7	14.2	17161
Al	60	20	9.0	13.0	1.2	392	26.6	9.5	12707
Al	60	60	11.5	14.5	0.58	153	26.2	9.3	10388
Al	60	40[a]	9.5	14.5	0.76	849	21.2	7.5	16732
Ba/Al	60	40	8.5	12.5	0.11	150	25.0	8.9	8339

[a] 30% PBD was added into PFN.

increased to 10.3 cd/A and 5047 cd/m^2, respectively. The device efficiency and luminance were greatly enhanced and reached 35.7 cd/A and 17161 cd/m^2, respectively, when the PVK layer was further increased to 60 nm. On the other hand, the device performance is less sensitive to the change in thickness of the PFN blend layer. For example, keeping the PVK thickness constant at 60 nm, devices with PFN(Ir) thickness of 20, 40, and 60 nm showed a luminous efficiency of 26.6, 35.7, and 26.2 cd/A, respectively (Table 1). Data in Table 1 also indicate that cathode metal quenching is not an important issue for this type of device. For example, a device with a 60 nm PVK and a 20 nm PFN(Ir) layer exhibited a higher efficiency (26.6 cd/A) compared with 15.3 cd/A for the device with 40 nm PVK and 40 nm PFN(Ir) (same total thickness of (PVK+PFN(Ir) of 80 nm).

The current vs electric field curves of different devices configurations were compared in Figure 3. It can be seen that the devices with a PVK layer showed much higher current density than the single-layer device without a PVK layer. When 60 nm PVK layer was inserted between PEDOT and the EL layer, the current density increased by about 2 orders of magnitudes under the same electric field. Considering the PVK is a typical p-type material, the increased current should be mainly contributed by hole current. Thus, the inserted PVK layer enhanced hole-injection which made hole and electron currents more balanced, resulting in the higher device efficiency. On the other hand, the devices with Ba/Al cathode or with 30% PBD blended into the EL layer did not show apparent differences in current-electric field characteristics compared with device of PFN/Al cathode showing similar device performances (see Table 1). This indicates that PFN/Al device has similar electron injection as Ba/Al device regardless of presence of PBD additive (typical electron-transport materials) (16, 20).

Previously, we reported highly efficient green phosphorescence by using PFO as the host and PVK as anode interlayer with device structure of ITO/PEDOT/PVK/PFO:PBD:Ir(Bu-PPy)$_3$/Ba/Al (21), where we revealed that the PVK layer played an important role in improving device performances through increasing hole injection and interlayer energy transfer. Similarly in this case when PFN was used as the host, the fact that very low device efficiency for Ir(Bu-PPy)$_3$ doped into PFN host might be partially due to the low-lying triplet level of PFN. Figure 4 compares the PL spectra of PFN doped with 4 wt % Ir(Bu-PPy)$_3$ in a single-layer film and a bilayer film with a 60 nm layer PVK underneath. When there was no PVK layer inserted, the PL spectrum shows only

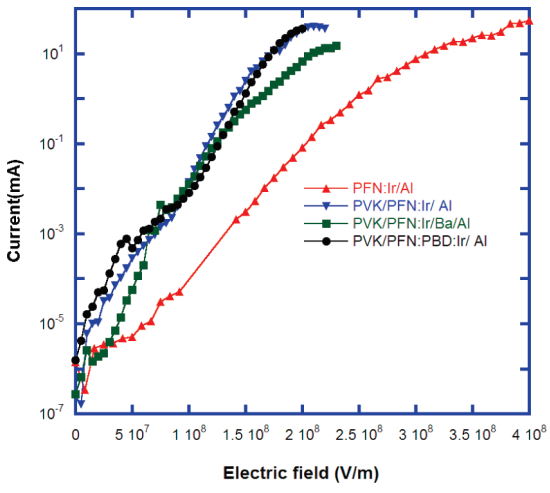

FIGURE 3. Current vs electric field of devices with different device configurations.

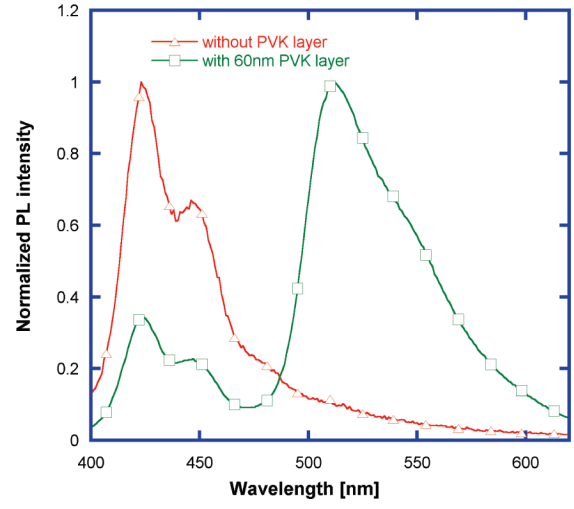

FIGURE 4. PL spectra of 4 wt % Ir(Bu-PPy)$_3$ doped in PFN with and without PVK layer.

the emission of PFN with peak at around 423 and 446 nm, and no guest emission was detected. However, when a layer of PVK was inserted between the substrate and the PFN-Ir blend layer, the emission of the Ir complex was greatly enhanced. This phenomenon was well-consistent with what we observed in PFO-Ir complex films (21). As we discussed for multilayer devices with a PVK/PFO(Ir)/Ba configuration, PVK plays hole-injection and electron-blocking layer. The LUMO of PFN and PVK is around 2.2(15) and 2.0 eV, respectively. As a result, there is a 0.2 eV barrier for electrons between the PFN/PVK interface and thus PVK acts as an electron-blocking layer. Because of the efficient electron injection and transport properties of PFN/Al, the recombination zone would be located close to the PVK side and electrons would be accumulated in the PVK/PFN interface. On the other hand, the HOMO level of the Ir complex is much higher than the PVK level, holes injected from a PVK layer are readily trapped by Ir complexes located in the PVK/PFN interface and recombine with electrons injected from the PFN/Al interface and accumulated in the PVK/PFN interface region. We note that because recombination takes place on the PVK/PFN interface, the back transfer of excitons in Ir complex-doped PFN blend (Figure 4) could be significantly retarded. Under such a mechanism, it is easy to understand why device efficiency increases with increasing PVK thickness. Clearly, as the PVK layer becomes thicker, the recombination zone moves closer to the PVK/PFN interface and the probability of recombination in the PFN bulk is reduced. Thus, we show that highly efficient green phosphorescence can be realized by using a more stable high work-function cathode such as Al without adding electron-transport materials (such as PBD).

CONCLUSIONS

In summary, efficient green-emitting phosphorescent PLEDs with a high work-function metal cathode of Al have been demonstrated by using PFN as host and PVK as anode interlayer. Device efficiency is sensitive to PVK thickness. When the thickness of PVK layer and the light-emitting layer was 60 and 40 nm, respectively, the highest luminance efficiency of 35.7 cd/A and maximum luminance of 17161 cd/m^2 were obtained. The high efficiency was realized because of the effective electron injection from Al to PFN, better charge balance, as well as a significant reduction of back-transfer from Ir complex to the low-lying PFN triplet level due to moving the recombination zone to the PVK/PFN interface. In addition, the use of this new device configuration (PVK/PFN(Ir)/Al) excludes the need for added electron-transport materials (such as PBD), thereby avoiding the potential problems arising from phase separation in the active layer. Investigation and comparative studies on stress life of these devices are in progress and will be reported in a forthcoming paper.

Acknowledgment. The work was financially supported by the National Natural Science Foundation of China (50990065, U0634003) and the Ministry of Science and Technology, China (MOST) National Research Project (2009CB623601).

REFERENCES AND NOTES

(1) Gong, X.; Lim, S. H.; Ostrowski, J. C.; Moses, D.; Bardeen, C. J.; Bazan, G. C. *J. Appl. Phys.* **2004**, *95*, 948–953.
(2) Wu, H. B.; Zou, J. H.; Liu, F.; Wang, L.; Mikhailovsky, A.; Bazan, G. C.; Yang, W.; Cao, Y. *Adv. Mater.* **2008**, *20*, 696–702.
(3) Hu, B.; Karasz, F. E. *J. Appl. Phys.* **2003**, *93*, 1995–2001.
(4) Jin, S.-H.; Kim, M.-Y.; Kim Jin, Y.; Lee, K.; Gal, Y.-S. *J. Am. Chem. Soc.* **2004**, *126*, 2474–2480.
(5) Lee, R.-H.; Hsu, H.-F.; Chan, L.-H.; Chen, C.-T. *J. Appl. Polym. Sci.* **2008**, *109*, 2605–2615.
(6) Quan, S.; Teng, F.; Xu, Z.; Qian, L.; Wang, Y. *Solid-State Electron.* **2006**, *50*, 1506–1509.
(7) Shaheen, S. E.; Jabbour, G. E.; Kippelen, B.; Peyghambarian, N.; Anderson, J. D.; Marder, S. R.; Armstrong, N. R.; Bellmann, E.; Grubbs, R. H. *Appl. Phys. Lett.* **1999**, *74*, 3212–3214.
(8) Heeger, A. J.; Parker, I. D.; Yang, Y. *Synth. Met.* **1994**, *67*, 23–29.
(9) Cao, Y.; Yu, G.; Parker, I. D.; Heeger, A. J. *J. Appl. Phys.* **2000**, *88*, 3618–3623.
(10) Xu, F.; Wang, C.; Yang, L.; Yin, S.; Wedel, A.; Janietz, S.; Krueger, H.; Hua, Y. *Synth. Met.* **2005**, *152*, 221–224.
(11) Brown, T. M.; Friend, R. H.; Millard, I. S.; Lacey, D. J.; Burroughes, J. H.; Cacialli, F. *Appl. Phys. Lett.* **2000**, *77*, 3096–3098.
(12) Fung, M. K.; Lai, S. L.; Tong, S. W.; Chan, M. Y.; Lee, C. S.; Lee, S. T.; Wu, W. W.; Inbasekaran, M.; O'Brien, J. J. *Appl. Phys. Lett.* **2002**, *81*, 1497–1499.
(13) Huang, J.; Xu, Z.; Yang, Y. *Adv. Funct. Mater.* **2007**, *17*, 1966–1973.
(14) Huang, F.; Hou, L.; Wu, H.; Wang, X.; Shen, H.; Cao, W.; Yang, W.; Cao, Y. *J. Am. Chem. Soc.* **2004**, *126*, 9845–9853.
(15) Huang, F.; Wu, H.; Wang, D.; Yang, W.; Cao, Y. *Chem. Mater.* **2004**, *16*, 708–716.
(16) Wu, H.; Huang, F.; Mo, Y.; Yang, W.; Wang, D.; Peng, J.; Cao, Y. *Adv. Mater.* **2004**, *16*, 1826–1830.
(17) Xu, Y.; Liang, B.; Peng, J.; Niu, Q.; Huang, W.; Wang, J. *Org. Electron* **2007**, *8*, 535–639.
(18) Dedeian, K.; Djurovich, P. I.; Garces, F. O.; Carlson, G.; Watts, R. J. *Inorg. Chem.* **1991**, *30*, 1685–1687.
(19) Bulovic, V.; Khalfin, V. B.; Gu, G.; Burrows, P. E.; Garbuzov, D. Z.; Forrest, S. R. *Phys. Rev. B* **1998**, *58*, 3730–3740.
(20) Wu, H. B.; Huang, F.; Peng, J.; Cao, Y. *Org. Electron.* **2005**, *6*, 118–128.
(21) Chen, Z.; Jiang, C.; Niu, Q.; Peng, J.; Cao, Y. *Org. Electron.* **2008**, *9*, 1002–1009.

AM9005258